JOC The Journal of Organic Chemistry

Article

pubs.acs.org/joc

A Lithium Amide Protected Against Protonation in the Gas Phase: Unexpected Effect of LiCl

Denis Lesage,[†] Gabriella Barozzino-Consiglio,[‡] Romain Duwald,[‡] Catherine Fressigné,[‡] Anne Harrison-Marchand,[‡] Kym F. Faull,[⊥] Jacques Maddaluno,[‡] and Yves Gimbert*[,§]

[†]Sorbonne Universités, UPMC UNIV Paris 06, Institut Parisien de Chimie Moléculaire, UMR CNRS 8232, Case 45, 4 Place Jussieu, 75252 Paris Cedex 05, France

[‡]Normandie Université (COBRA), UMR CNRS-Université de Rouen-INSA de Rouen 6014, 76821 Mont St Aignan Cedex, France

[§]Université Grenoble Alpes (DCM), UMR CNRS-UJF 5250 BP 53, 38041 Grenoble Cedex 9, France

[⊥]Pasarow Mass Spectrometry Laboratory, Semel Institute for Neuroscience and Human Behavior and Department of Psychiatry and Biobehavioral Sciences, David Geffen School of Medicine at UCLA, Los Angeles, California, 90019 United States

Supporting Information

ABSTRACT: In cold THF and in the presence of LiCl, a lithium pyrrolidinylamide forms a 1:1 mixed aggregate, which is observed directly by ESI-MS. Gas-phase protonation of this species leads to selective transfer of H^+ to the chlorine, suggesting that LiCl shields the amide nitrogen and prevents its direct protonation.

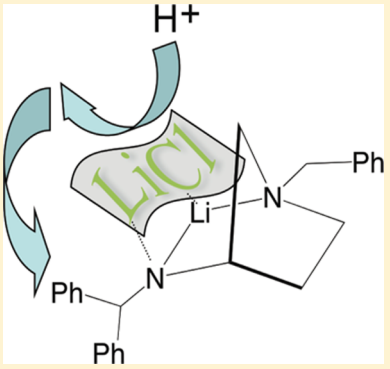

INTRODUCTION

Lithium chloride occupies a distinctive position in organometallic chemistry. Known for decades for impacting the reactivity of organolithium and organomagnesium derivatives, this salt has a multitude of other important effects.[1] For instance, LiCl improves the solubility of less soluble lithium derivatives and is also critical for attaining efficient metalation processes,[2a] including useful levels of both enantioselectivity in deprotonations with chiral lithium amides[2b] and chemoselectivity of turbo-Grignard reagents.[3]

Attempts have been made to explain the molecular basis for the effects of this salt, but only empirical or *ad hoc* models, often developed solely to account for specific results, have been proposed to date. Sophisticated analytical tools that have recently become available, however, have now allowed a degree of clarification concerning the role of inorganic adjuncts in a number of other cases. Frequently, a mixed aggregate associating the reactant and the salt is identified, the structure of which can vary as a function of the exact experimental conditions.[4]

The influence of LiCl on lithium amides is of particular interest because these "utility reagents"[5] are often contaminated by traces of inorganic salts (e.g., lithium halides from the alkyl lithium reagents used to deprotonate the amine) with which they can readily form mixed aggregates. Although some of these entities have been reasonably well characterized, mainly through X-ray crystallography or NMR,[4] their dynamic behavior is far from clear; the available data offer only descriptions and fail to provide any predictive assessment of the reactivity of these complexes.

RESULTS AND DISCUSSION

In this context, we focused on a lithium pyrrolidinylamide, **1-Li** (Scheme 1). This chiral amide, obtained by deprotonation of **1-H**, was selected because of its remarkable features. For instance, it associates spontaneously and completely with different lithium derivatives to exclusively form 1:1 noncovalent but stable mixed aggregates in THF.[6] These complexes exhibit

Scheme 1. Synthesis and Structure of the 1-Li/LiCl Mixed Aggregate in THF

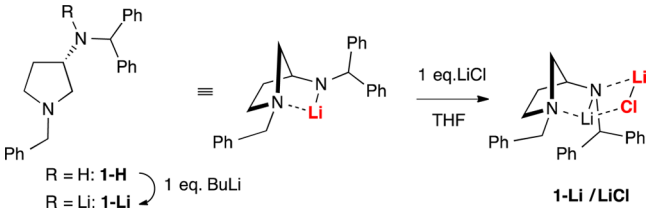

Received: April 20, 2015
Published: May 21, 2015

DOI: 10.1021/acs.joc.5b00875
J. Org. Chem. 2015, 80, 6441−6446

good nucleophilic properties, and in several cases, the partner of the amide has been shown to add onto the carbonyl of aldehydes with medium to high enantioselectivities (50−85% ee).

Aggregations have been observed with sp^3, sp^2, as well as sp organolithium derivatives; thus, aminopyrrolidines (**1-H**) can be regarded as relatively general chiral auxiliaries. Several of these complexes have been fully characterized by NMR, in particular through bidimensional HOESY and ^{1}H-DOSY experiments.[7] If the orientation and the connections between the partners as well as their solvation are now well understood, evaluating the reactivity of such highly reactive entities by NMR remains complex.[8]

Mass spectrometry, which has proven to be a valuable tool for elucidating various supramolecular organometallic structures and studying their reactivity in the gas phase,[9] seemed to offer a possible means to examine the interaction of mixed aggregates of **1-Li** with an electrophile. This has indeed proven to be feasible and is described below.

Mass Spectrometry Experiments. Finding appropriate ionization conditions that conserve an aggregate structure from the solution phase to gas phase a priori is not a trivial issue. This is the reason why, to increase our chance to perform such a transfer, the robust solvated **1-Li/LiCl** complex, previously well characterized in THF solution by NMR and DFT (Scheme 1),[10] was selected for study. A proton was chosen as a canonical model electrophile. In addition to furnishing structural information on the aggregate, including its solvation in the gas-phase (which can be anticipated to be different from solution), mass spectrometry was expected to provide insight into the relative affinities for H^+ of the two basic sites (the nitrogen atoms) in the **1-Li/LiCl** complex. Our preliminary results, as well as data published recently on related problems,[11] suggests that electrospray ionization (ESI) could be an appropriate technique for studying this complex in the gas-phase.

Complex **1-Li/LiCl** was prepared by deprotonation of amine **1-H** in THF at −20 °C with *n*-BuLi, followed by the addition of an equimolar amount of LiCl in dry THF (Scheme 1). The concentration in Li derivatives in THF solution are in agreement with the standard conditions to perform this kind of organolithium transformation, imposing the necessity of dilution before being introduced to the ESI source. Thus, this solution, still at −20 °C, was diluted in dry THF to ∼10^{-5} M, anticipating that this dilution conserves the **1-Li/LiCl** structure solvated by THF. All spectra were recorded in the positive-ion mode.

The ESI-MS spectrum of this solution showed a peak at *m*/*z* 463, corresponding to [**1-Li/LiCl** + 1THF + H]$^+$ and not the expected [**1-Li/LiCl** + 1THF + Li]$^+$. Protonation takes place in solution during the electrospray ionization process, and MS/MS experiments of the resulting protonated aggregate were examined. A series of collision induced dissociation (CID) studies (Figure 1, left) on this parent ion were performed next at different collision voltages. At 12 V, fragments at *m*/*z* 391 and 349 were produced, which correspond to the [**1-Li/LiCl** + H]$^+$ and [**1-Li** + H]$^+$ (or [**1-H** + Li$^+$]) ions, respectively. At 25 V, the fragment ion at *m*/*z* 391 was no longer present, and only the peak at *m*/*z* 349 was observed. At 50 V, the fragment at *m*/*z* 349 persisted, but a new ion at *m*/*z* 91 (Bn^+) was also produced. When the ^{37}Cl isotope was selected (CID on the parent at *m*/*z* 465), the fragment at *m*/*z* 391 was shifted to 393, whereas that at *m*/*z* 349 was, as expected, unchanged. This

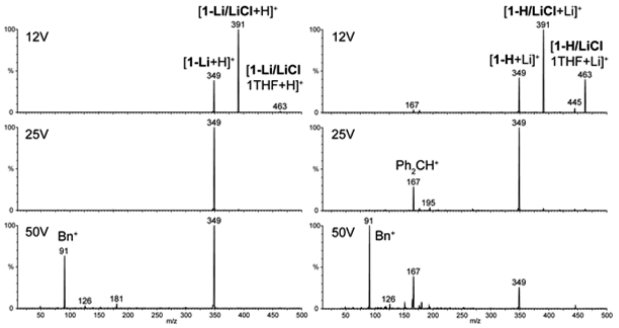

Figure 1. CID spectra at various collision energies (top, 12 V; middle, 25 V; bottom, 50 V) of the preselected parent ion at *m*/*z* 463, produced from [**1-Li/LiCl** + 1THF + H]$^+$ (left column), and from [**1-H/LiCl** + 1THF + Li]$^+$ (right column).

fragmentation pattern suggested a loss of THF (*m*/*z* 391) and then of LiCl (*m*/*z* 349). The observation of only one solvating THF in the gas phase is in line with the solvation energies previously calculated.[12] It is worth noting that the departure of LiCl occurs after that of THF.

At this stage, it was postulated that the structure of the ion at *m*/*z* 463 might correspond to reprotonation of amide **1-Li** to generate amine **1-H**, which, complexed with LiCl, then associated with Li$^+$ (i.e., [**1-H** + LiCl + 1THF + Li$^+$]). In an attempt to verify this possibility, the CID experiment (Figure 1, right) was repeated, but now starting from amine **1-H** (same LiCl concentration; solution injected under the same protocol). The previous peaks (*m*/*z* 463, 391, and 349) were produced, together with a new peak at *m*/*z* 167, which corresponded to the benzhydrylium (Ph_2CH^+) cation. Whereas the peak at *m*/*z* 91 suggested that the ring nitrogen had been protonated (Scheme 2), that at *m*/*z* 167 seemed to imply protonation of

Scheme 2. Proposed Formation of Fragments at *m*/*z* 91 and 167 from [1-H + H]$^+$

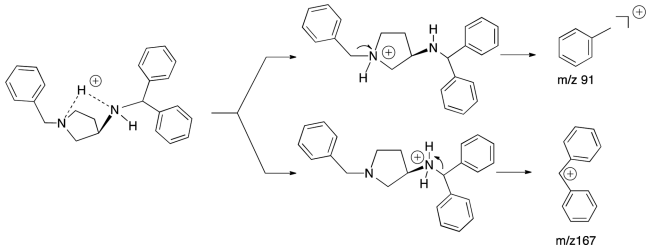

the exocyclic nitrogen. The peak at *m*/*z* 167 was not observed in the MS/MS spectrum of the ion at *m*/*z* 463, which was obtained starting from the **1-Li** solution.[13]

The difference between these spectra was puzzling because, starting a priori from the same complex, exactly the same spectra should have resulted, which raises the question, do the ions at *m*/*z* 463 actually have the same structure when generated from the **1-Li** and **1-H** solutions?

DFT Studies. To gain insight into this interesting gas-phase fragmentation divergence, a DFT study at the B3P86/6-31+G(d,p) level, previously benchmarked on this type of structure,[10] was performed. The solvent was taken into account through a PCM continuum procedure (single point calculation) but only for the ions resulting from the initial protonation phenomenon that occurs inside the droplet during the spraying process. For the fragments resulting from CID processes, the

DOI: 10.1021/acs.joc.5b00875
J. Org. Chem. 2015, 80, 6441−6446

PCM is not relevant because the fragmentation occurs after volatilization (i.e., in the vacuum of the collision cell).

We first decided to evaluate the influence of LiCl on the proton affinity of each nitrogen atom. A set of calculations was thus run on **1-Li** alone with the PCM included. As expected, the protonation of the exocyclic amide nitrogen yields a regioisomer more stable than the one corresponding to a protonation on the intracyclic tertiary amine nitrogen by more than 26 kcal/mol. The situation is similar when starting from **1-Li/LiCl**, the difference between the two protonation sites exceeds 25 kcal/mol in favor of the same exocyclic nitrogen.

The subsequent computational step focused on the protonation of [**1-Li** + 1THF], which is the supermolecule detected by MS. This 2-fold modeling of the solvation (discrete + continuum) is expected to reflect the presence of a lithium coordinated solvent molecule strongly bound to the lithium in addition to the dynamic solvation shell.

Protonation of the exocyclic nitrogen restores the original N−H bond and leads to a $[\mathbf{1\text{-}H} + 1THF + Li]^+$ minimum in which the Li cation is chelated by the two nitrogen atoms (Scheme 3). Protonation of the endocyclic nitrogen leads to

Scheme 3. Modeling of $[\mathbf{1\text{-}Li} + THF + H]^+$[a]

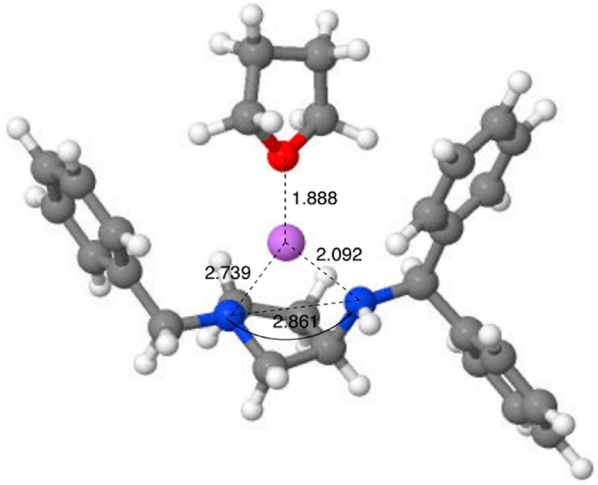

[a]Distances are in Å (N in blue, Li in purple, O in red).

the same structure spontaneously upon optimization. This result is consistent with the basicity difference between the N−Li amide and the N−Bn amine mentioned above.

Next, the [**1-Li/LiCl** + 1THF] structure (Scheme 4a) was optimized. Calculations led to a mixed aggregate with two main interactions: one between the lithium cation of LiCl and the nitrogen of the amide, the other between the chloride of LiCl and the lithium of the N−Li appendage. As a consequence of these interactions, the Li−Cl bond is lengthened (2.22 Å in the complex vs 2.06 Å in free LiCl).

As with [**1-Li** + 1THF], the two nitrogen atoms in [**1-Li/LiCl** + 1THF] remain in the expected protonation sites. In contrast to the results in the absence of LiCl, however, protonation of the ring nitrogen now leads to a local minimum, probably due to a secondary H−Cl interaction with the nearby chloride. However, this regioisomer is 27 kcal mol^{-1} (24 with the PCM contribution) less favored than the exocyclic isomer (Scheme 4b). Kinetic protonation of one of the nitrogen atoms was considered next because the mass spectrometric conditions tend to favor kinetic phenomena. A possible trajectory was

Scheme 4. Optimized Structure of (a) [1-Li/LiCl + 1THF] Alone and (b) [1-Li/LiCl + 1THF] + H^+[a]

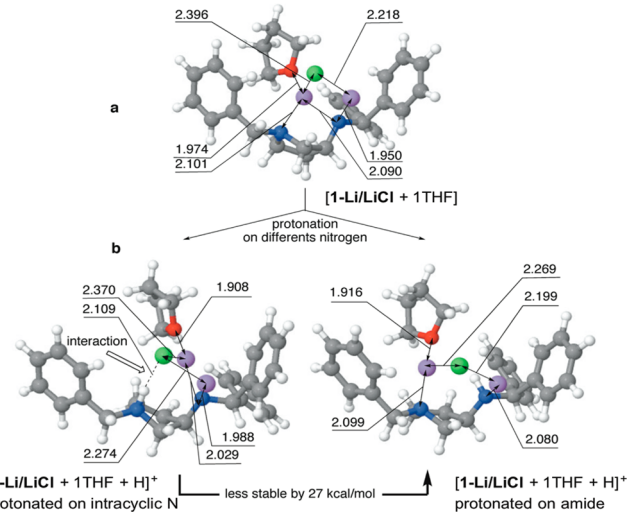

[a]Distances are in Å (N in blue, Li in purple, O in red, Cl in green).

qualitatively simulated by successively approaching the nitrogen atoms with an H^+, starting sufficiently distant for the proton to be able to completely explore the space around the target atom (see Scheme 5). However, this proved initially problematic because the Li^+ around the nitrogens tended to deflect the oncoming proton due to Li + H^+ electrostatic repulsion.

This problem could be circumvented through a two-stage study: First, the proton was frozen at ≈3.6 Å from one of the two nitrogens while local minima were sought (Phase I). Setting the distance between a nitrogen atom and a H^+ cannot provide a significant value for the energy; however, this procedure can give trends about the gradients undertaken by a proton in its environment. This "braced" optimization led to two different structures separated by only 2.4 kcal mol^{-1} with the complex in which the H^+ approaches the lithium amide favored (route (ii)).

Beyond the approximate energy difference between these two structures, it is worth mentioning that the two starting points both led to the initial formation of HCl, as shown in Scheme 5. This suggested that the primary protonation site of the complex was the chloride, which enjoys enhanced basicity because of the partial dissociation produced by diamine coordination of the Li counterion.[14]

As a result, HCl would be the actual protonating agent in this system. It should be recognized that the highly negative-potential electrostatic zone calculated around the chloride is fully consistent with this interpretation (see the Supporting Information).

The next computational stage (Phase II) involved the N−H separation being allowed to vary in these two minima, which unexpectedly generated a unique $[\mathbf{1\text{-}Li} + 1THF + HCl + Li]^+$ optimized aggregate. Remarkably, no nitrogen was protonated because the two Li cations shielded them from the incoming H^+. The excluded HCl molecule, however, does interact through its proton with one of the aromatic rings (Scheme 6). However, it should be kept in mind that the $[\mathbf{1\text{-}Li} + 1THF + HCl + Li]^+$ complex is a kinetic product that is considerably less stable than the complexes resulting from protonation of the *endo*- or *exo*-cyclic nitrogen atoms (by 27 and 56 kcal/mol, respectively). Although the calculations suggested that the ion

DOI: 10.1021/acs.joc.5b00875
J. Org. Chem. 2015, 80, 6441−6446

Scheme 5. Successive Structures Calculated During the Approach of the Endocyclic (Route (i)) and Exocyclic (Route (ii)) Nitrogen Atom of [1-Li/LiCl + 1THF] by a Proton[a]

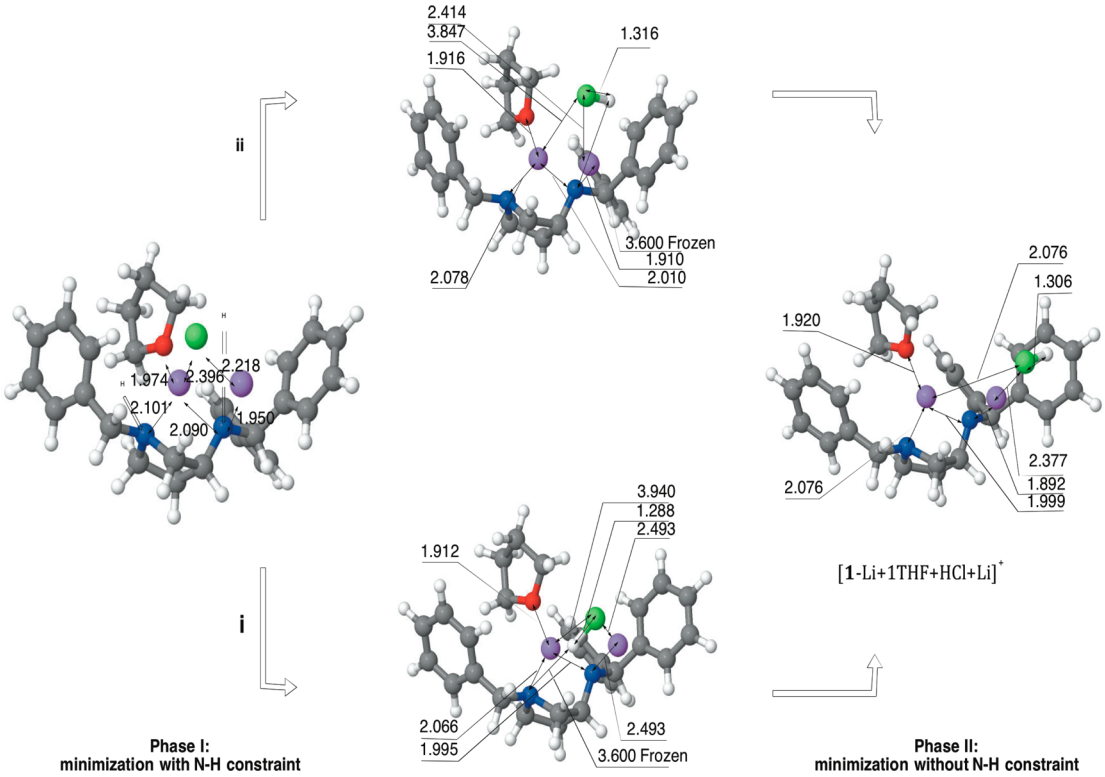

[a]Phase I: frozen N−Li distance. Phase II: fully relaxed optimization. Distances are in Å (N in blue, Li in purple, O in red, Cl in green).

Scheme 6. Structure of [1-Li + HCl + Li]$^+$ Ion Corresponding to the Peak at *m/z* 391 (left) and of [1-Li + H]$^+$ Ion Corresponding to the Peak at *m/z* 349 (right)[a]

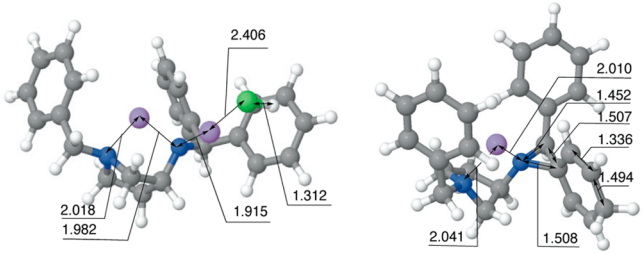

[a]Distances are in Å (N in blue, Li in purple, O in red, Cl in green).

formed at *m/z* 463 [**1-Li** + 1THF + HCl + Li]$^+$ was that depicted in Scheme 5, it was difficult to understand why this complex in the CID experiment did not immediately lose HCl but instead first released THF and then LiCl. Thus, exactly how, under these conditions, the proton could undergo transfer to one of the two nitrogens remained unclear. To tackle this question, an effort was made first to identify the structure of the ions at *m/z* 391 and 349 and then to determine if the departure of THF, followed by LiCl, could trigger a proton transfer to one of the nitrogens.

The calculations were thus repeated on the [**1-Li** + HCl + Li]$^+$ aggregate (corresponding to *m/z* 391, obtained by removing the THF from the optimized [**1-Li** + 1THF + HCl + Li]$^+$). The optimization led to a structure in which the two nitrogens coordinate one of the two Li atoms (Scheme 6, left). However, at this stage, no proton transfer was expected. The next peak at *m/z* 349 corresponded to the loss of LiCl. This elimination was calculated with the involvement of the two different Li atoms of the above [**1-Li** + HCl + Li]$^+$ complex. The optimizations indicated that proton transfer indeed takes place here but not toward either of the nitrogen atoms; instead, the proton interacts with the para carbon of one of the phenyls of the benzhydryl group. This is reminiscent of the proton of HCl in the [**1-Li** + 1THF + HCl + Li]$^+$ complex, which is oriented toward a para carbon (Scheme 4). The phenyl is finally dearomatized and affords a spiroaziridine (Scheme 6, right). This unexpected structure was systematically obtained after optimization, and any Li was removed with the Cl.

The possibility that HCl could be effecting protonation through an intermediate proton transfer to the oxygen of the THF has also been considered. This isomeric complex is only 5 kcal/mol less stable than the starting point; however, calculations showed that this stable minimum does not evolve spontaneously toward the protonation of a nitrogen (see the Supporting Information).

CONCLUSION

In summary, in the gas phase, the mixed aggregate **1-Li/LiCl** appears to adopt a 1:1 structure similar to that established in THF solution by multinuclear NMR. The MS data show that cationization relies on one proton and not on Li$^+$. The DFT studies ran in parallel suggest that, surprisingly, the basicity of the chloride is strongly enhanced in the gas-phase (see Scheme 7 for a schematic representation of the whole protonation process). Thus, it becomes the primary (kinetic) site for protonation, which leads to the formation of HCl (the nitrogens are the thermodynamic sites). This behavior is obviously quite different from that in solution, where the

DOI: 10.1021/acs.joc.5b00875
J. Org. Chem. 2015, 80, 6441−6446

Scheme 7. Representation of the Protonation Process of the Aggregate 1-Li/LiCl in the Gas Phase[a]

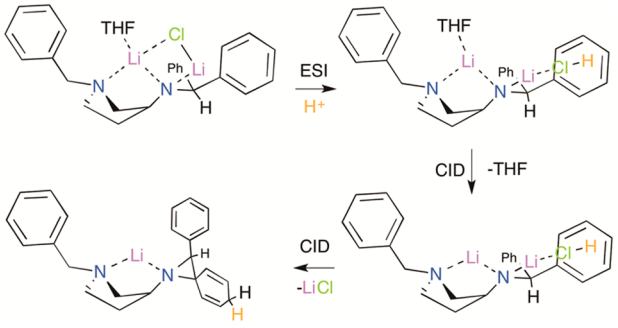

[a]ESI, electrospray ionization; CID, collision induced dissociation.

strongly basic amide nitrogen immediately captures the proton. Calculations indicate that, in the gas-phase, the final destination of the proton is the para carbon of a phenyl group of the benzhydryl appendage. Overall, LiCl thus protects lithium amide **1-Li** from direct protonation and thereby demonstrates a salt effect never before observed.

EXPERIMENTAL SECTION

Synthesis of 1-Li/LiCl. *General Considerations.* Synthetic manipulations were carried out in oven-dried glassware under an atmosphere of anhydrous and deoxygenated argon. Argon was dried and deoxygenated by bubbling through a commercial solution of *n*-BuLi in hexanes. THF was carefully distilled upon benzophenone/sodium and degassed by bubbling dry argon to produce water, oxygen, and peroxide-free THF. The water content in these conditions is ≈10 ppm, ensuring a limited, internal source of protons. LiCl was dried under high vacuum for 24 h at 140 °C. After cooling to room temperature, LiCl was dissolved in freshly distilled THF to obtain a 0.3 M solution. Aminopyrrolidine **1-H** was synthesized according to the procedure reported in the literature.[15]

Synthesis of 1-Li/LiCl Mixed Aggregate. Under an argon atmosphere, *n*-BuLi (1.6 M solution in hexanes, 0.5 mL, 0.75 mmol) was added dropwise to a solution of **1-H** (257 mg, 0.75 mmol) in freshly distilled and deoxygenated THF (15 mL) at −20 °C. After being stirred for 20 min, a 0.3 M solution of anhydrous LiCl (2.5 mL, 0.75 mmol) was added to the preformed solution of **1-Li**, and the resulting mixture was stirred for 30 min at −20 °C. Then, the **1-Li/LiCl** complex was kept at −78 °C prior to use.

Mass Spectrometry Experiments. Triple-quadrupole experiments were performed using a mass spectrometer equipped with a Z-spray source. ESI solutions were introduced into the mass spectrometer using a microreactor in order to achieve a dilution of Li/LiCl in THF of ∼10^{-5} M. The cold starting solution, prepared as described above, is introduced by a first entry into the microreactor via a syringe pump operating at 240 μL/h, and THF is introduced via an HPLC system at a fixed flow rate of 3000 μL/h; the solvent is precooled to −30 °C just before the second entry of the microreactor. The exit of the reactor is directly connected to the source. The ESI capillary voltage is maintained at 3.5 kV, and the cone voltage varies from 10 to 60 V (positive mode). Nitrogen was used as the desolvation and nebulization gas. The source and desolvation temperatures were kept at 120 and 100 °C, respectively.

ASSOCIATED CONTENT

Supporting Information

Scheme of the device using a microreactor for mass spectrometry experiments, MS spectra of (**1-Li**/LiCl) and (**1-H**/LiCl) solution, energy-resolved mass spectra (ERMS) of [1-H]$^+$, computational details, and Cartesian coordinates for all of the molecules reported in this study. The Supporting Information is available free of charge on the ACS Publications website at DOI: 10.1021/acs.joc.5b00875.

AUTHOR INFORMATION

Corresponding Author

*E-mail: Yves.Gimbert@ujf-grenoble.fr.

Notes

The authors declare no competing financial interest.

ACKNOWLEDGMENTS

We are grateful to the CNRS for a postdoctoral fellowship (G.B.), and to the CRIHAN and CECICCLUSTER for computational support.

REFERENCES

(1) Hevia, E.; Mulvey, R. E. *Angew. Chem., Int. Ed.* **2011**, *50*, 6448−6450.

(2) (a) For accelerating effects on the metallating ability of LDA, see: Gupta, L.; Hoepker, A. C.; Singh, K. J.; Collum, D. B. *J. Org. Chem.* **2009**, *74*, 2231−2233. (b) For recent reviews, see: Davies, S. G.; Fletcher, A. M.; Roberts, P. M.; Thomson, J. E. *Tetrahedron: Asymmetry* **2012**, *23*, 1111−1150. Simpkins, N. S.; Weller, M. D. *Org. React.* **2013**, *79*, 317−635. Harrison-Marchand, A.; Maddaluno, J. In *Lithium Compounds in Organic Synthesis: From Fundamentals to Applications*; Luisi, R., Capriati, V., Eds.; Wiley-VCH: Weinheim, Germany, 2014.

(3) For examples, see: (a) Krasovskiy, A.; Knochel, P. *Angew. Chem., Int. Ed.* **2004**, *43*, 3333−3336. (b) Piller, F. M.; Appukkuttan, P.; Gavryushin, A.; Helm, M.; Knochel, P. *Angew. Chem., Int. Ed.* **2008**, *47*, 6802−6806. (c) Knochel, P.; Gavryushin, A.Lithium Dichloro(1-methylethyl)-magnesate. In *Encyclopedia of Reagents for Organic Synthesis*; John Wiley & Sons: New York, NY, 2010.

(4) For recent reviews, see: (a) Reich, H. J. *Chem. Rev.* **2013**, *113*, 7130−7178. (b) Harrison-Marchand, A.; Mongin, F. *Chem. Rev.* **2013**, *113*, 7563−7727.

(5) Mulvey, R. E.; Robertson, S. D. *Angew. Chem., Int. Ed.* **2013**, *52*, 11470−11487.

(6) (a) Paté, F.; Gérard, H.; Oulyadi, H.; de la Lande, A.; Harrison-Marchand, A.; Parisel, O.; Maddaluno, J. *Chem. Commun.* **2009**, 319−321. (b) Lecachey, B.; Fressigné, C.; Oulyadi, H.; Harrison-Marchand, A.; Maddaluno, J. *Chem. Commun.* **2011**, *47*, 9915−9917. (c) Harrison-Marchand, A.; Gérard, H.; Maddaluno, J. *New J. Chem.* **2012**, *36*, 2441−2446.

(7) For recent applications of this technique to organometallic derivatives see: (a) Li, D; Kagan, G.; Hopson, R.; Williard, P. G. *J. Am. Chem. Soc.* **2009**, *131*, 5627−5634. (b) Guang, J.; Li, W.; Wu, K.; Hopson, R.; Williard, P. G. *J. Am. Chem. Soc.* **2014**, *136*, 11735−11747. (c) Hamdoun, G.; Sebban, M.; Cossoul, E.; Harrison-Marchand, A.; Maddaluno, J.; Oulyadi, H. *Chem. Commun.* **2014**, *50*, 4073−4075.

(8) For a remarkable example, see: Jones, A. C.; Sanders, A. W.; Sikorski, W. H.; Jansen, K. L.; Reich, H. J. *J. Am. Chem. Soc.* **2008**, *130*, 6060−6061.

(9) (a) *Reactive Intermediates*; Santos, L. S., Ed.; Wiley-VCH: Weinheim, Germany, 2010. (b) Tian, Z.; Kass, S. R. *Chem. Rev.* **2013**, *113*, 6986−7010. (c) Simonneau, A.; Jaroschik, F.; Lesage, D.; Karanik, M.; Malacria, M.; Tabet, J.-C.; Goddard, J.-P.; Fensterbank, L.; Gandon, V. *Chem. Sci.* **2011**, *2*, 2417−2422. (d) Lesage, D.; Milet, A.; Memboeuf, A.; Blu, J.; Greene, A. E.; Tabet, J.-C.; Gimbert, Y. *Angew. Chem., Int. Ed.* **2014**, *53*, 1939−1942.

(10) Paté, F.; Duguet, N.; Oulyadi, H.; Harrison-Marchand, A.; Fressigné, C.; Valnot, J.-Y.; Lasne, M.-C.; Maddaluno, J. *J. Org. Chem.* **2007**, *72*, 6982−6992.

(11) For a recent observation using an ESI-MS approach of a remarkable molecular salt effect on the basicity of organometallic species, see: Khairallah, G. N.; da Silva, G.; J. O'Hair, R. A. *Angew. Chem., Int. Ed.* **2014**, *53*, 10979−10983.

DOI: 10.1021/acs.joc.5b00875
J. Org. Chem. 2015, 80, 6441−6446

(12) Yuan, Y.; Desjardins, S.; Harrison-Marchand, A.; Oulyadi, H.; Fressigné, C.; Giessner-Prettre, C.; Maddaluno, J. *Tetrahedron* **2005**, *31*, 3325−3334.
(13) MS experiments are reported and discussed in the Supporting Information.
(14) Forti, L.; Ghelfi, F.; Pagnoni, U. M. *Tetrahedron Lett.* **1995**, *36*, 3023−3026.
(15) (a) Maddaluno, J.; Corruble, A.; Leroux, V.; Plé, G.; Duhamel, P. *Tetrahedron: Asymmetry* **1992**, *3*, 1239−1242. (b) Corruble, A.; Valnot, J.-Y.; Maddaluno, J.; Duhamel, P. *Tetrahedron: Asymmetry* **1997**, *8*, 1519−1523. (c) Corruble, A.; Valnot, J.-Y.; Maddaluno, J.; Duhamel, P. *J. Org. Chem.* **1998**, *63*, 8266−8275.

DOI: 10.1021/acs.joc.5b00875
J. Org. Chem. 2015, 80, 6441−6446